

Structure and morphology of chitosan / bioactive glass prepared by sol-gel method

Dalila KSOURI, Hafit HKIREDDINE, Ali AKSAS, Fatima BIR, Nadir SLIMANI

Laboratoire de Génie de l'Environnement (LGE), Faculté de Technologie, Département de Génie des Procédés,
Université de Bejaia, 06000 Bejaia, Algeria

Abstract — In this study, bioactive glass in ternary system composition $\text{SiO}_2\text{-CaO-P}_2\text{O}_5$ was synthesized via sol-gel method. The aim of this study is to add a biopolymer which is the chitosan to the solution of 63S bioactive glass. The sol obtained is mixed with a chitosan solution at different percentage (0%, 10%, 30%, 60% and 90%) then heated at 60°C for 10 h and drying at 130°C for 20 h. The powders sintered at 600°C for 2h and characterized by XRD, FTIR and SEM analyzes. The influence of the addition of chitosan on the structure and morphology of the bioactive glass powders was distinguished and the results showed that the bioactive glass powders have a crystalline structure with the increasing of chitosan rate and this is approved by the XRD and SEM analyses.

Keywords: *Biomaterials, bioactive glass, Sol-Gel method, Chitosan.*

I. INTRODUCTION

Significant interest has been generated in the application of synthetic bioactive materials in tissue engineering. Biomaterials can be produced from many kinds of materials, such as synthetic polymers, metals, ceramics and natural macromolecules that have the proper morphology and properties according to the application requirements [1]. This family of substitutes is particularly suitable for filling bone defects [2] as well as prosthetic coatings in orthopedic surgery, maxillofacial, aestheticians and dental [3, 4]. The main advantages of these synthetic biomaterials are availability, reproducibility and reliability. They must be biocompatible, they should not generate any complication or inflammatory response and also be suitable in their mineral compositions [5]. Hench and al [6] has reviewed the development of bioactive silicate glasses.

One of the most important reasons for welcoming these kinds of materials is their excellent biocompatibility [7], good bioactivity in comparison with metallic and polymeric biomaterial [8], their osteoconductivity and their biodegradability [9, 10]. In fact, in contact with living tissues, bioactive glasses generate a series of physical and chemical reactions material / bone tissue leading to the formation of hydroxyl carbonate apatite (HCA) layer interface [11, 12], which has a similar composition to the inorganic part of human bone [13, 14].

Sol-gel is the most widely used technique for synthesis of bioactive glass. Sol-gel derived bioactive glass, compared to traditional melt processed, has higher bioactivity and biodegradability [15].

In this investigation, we study the effect of the addition of chitosan, a kind of polysaccharide [16], which is acetylated derivative of chitin and has been widely applied in biomedical applications because of its cell compatibility, biodegradability and non-toxic characteristics [17], into the solution of ternary bioactive glass synthesized by sol-gel method. The structure and morphology of ternary

Corresponding author: Dalila KSOURI,
Research field: Biomaterials
Adress. LGE/ University of bejaia - Algeria
E-mail: dalidakso@gmail.com

bioactive glass with different rate of chitosan were studied.

II. Synthesis of chitosan / bioactive glass

SiO₂-CaO-P₂O₅ ternary bioactive glass was synthesized via sol-gel method [7]. Initially, tetraethylorthosilicate (TEOS) was added to ethanol as an alcoholic media and the mixture was stirred for 30 min. The following reagents were added in the following sequence, stirring 30 min for each reagent to react completely: the H₂O:TEOS molar ratio was 4:1, triethylphosphate (TEP), calcium nitrate tetrahydrate and hydrochloric acid (HCl, 2N).

After the final addition, the solution was stirred for one hour additional. Chitosan solution at a concentration of 2wt% was dissolved in 2% acetic acid. The sol was mixed with the chitosan solution at different volume ratios (chitosan at 0%, 10%, 30%, 60% and 90%) and the mixtures were stirred for 2 h, heated at 60°C for 10 h and dried at 130°C for 20 h. The final products were crushed then sintered at 600 °C for 2 h. The different powders of bioactive glass with and without chitosan noticed BG-0% Ch, BG-10% Ch, BG-30% Ch, BG-60% Ch and BG-90% Ch were characterized by XRD for phase analysis, FTIR for identification of functional groups and scanning electron microscopy (SEM) for the morphology.

III. Results and Discussion

III.1. Characterization of chitosan

III.1.1. XRD analysis of chitosan

X-ray diffraction pattern of chitosan is shown in Fig. 1. The diffractogram of chitosan shows characteristic peaks at 10.4° and 20.4° which coincides with the pattern of the ‘L-2 polymorph’ of chitosan [18].

The FTIR spectrum of chitosan is shown in Fig.2. The strong and broad band centered at 3440 cm⁻¹ which is attributed to the axial stretching of O-H and N-H bonds. The band corresponding to the axial stretching of C-H bonds is observed around 2889 cm⁻¹ and the

bands centered at 1650 cm⁻¹ and 1601 cm⁻¹ is assigned to the amide I and amide II vibrations, respectively. The spectrum show also two bands at 1422 cm⁻¹ and 1380 cm⁻¹ resulting from the coupling of C-N axial stretching and N-H angular deformation and the bands in the range 1088–897 cm⁻¹ due to polysaccharide skeleton, including the glycosidic bonds, C-O and C-O-C stretchings [19].

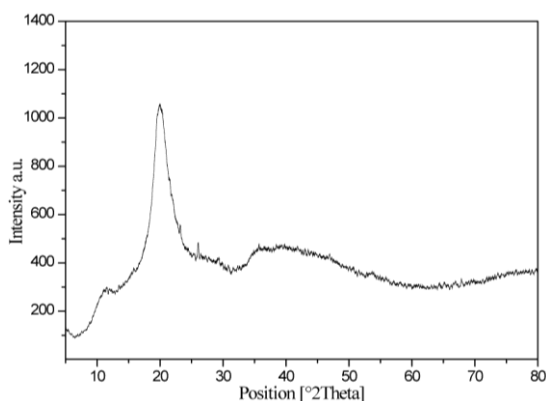


Fig. 1 The diffractogram of chitosan

III.1.2. FTIR analysis of chitosan

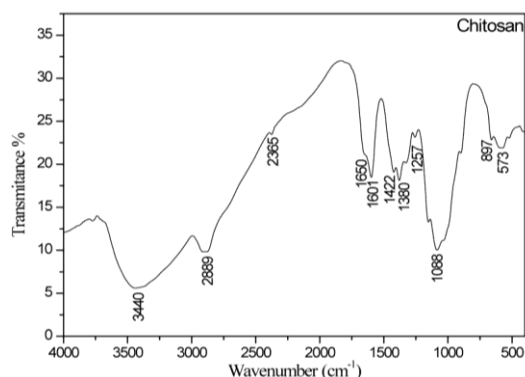


Fig.2 FTIR spectrum of chitosan

III.2. Characterization of bioactive glasses with the addition of chitosan

III.2.1. XRD analysis bioactive glasses

The X-ray diffraction analysis result for the bioactive glass with different rate of chitosan is shown in Fig.3. The samples BG-0% Ch, BG-10% Ch and BG-30% Ch shown the same

patterns, these samples takes amorphous state indicative of the intern disorder and glassy nature of these materials [10, 20]. We observed a crystalline structure in the samples with the rate of 60% and 9% of chitosan, these peaks can be assigned to the wallastonite (CaSiO_3) or to the apatite [21 - 23]. The crystallization process depending on the heat treatment conditions [24, 25]. Whereas, In this work we observed that the crystallization depends on the increasing of the rate of chitosan.

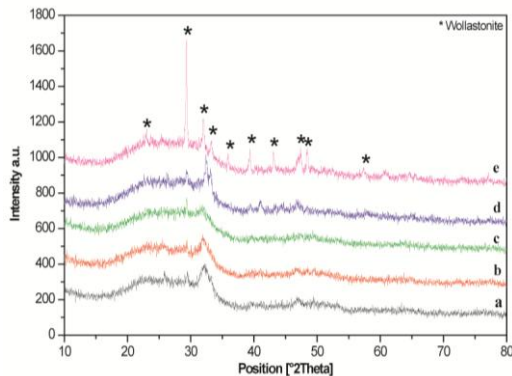


Fig. 3 The diffractograms of bioactive glass powders: (a) BG-0% Ch, (b) BG-10% Ch, (c) BG-30% Ch, (d) BG-60% Ch and (e) BG-90% Ch.

III.2.2. FTIR analysis of bioactive glasses

The effect of chitosan addition is studied by FTIR spectral analysis, which is shown in Fig. 4. The samples shown a strong absorption bands around 1058 cm^{-1} assigned to the Si-O-Si asymmetric bond stretching vibrations, this band became larger with the increasing of the percentage of chitosan especially in the case of 60 and 90 % of chitosan. The band in the 786 cm^{-1} is attributed to the symmetric Si-O-Si stretching vibrations [1, 21, 26] this band is almost disappeared for the bioactive glasses with 60 and 90 % of chitosan and the absorption around 455 cm^{-1} due to the vibrational mode of the bending of Si-O-Si [22, 24, 27] which prove that all the samples are mainly composed of a Si-O-Si network. The weak inflection at 1641 cm^{-1} and the broad band centered at 3473 cm^{-1} are assigned to O-H band of adsorbed water and structural hydroxyl group respectively [3, 4, 28] and finally the band at 1440 cm^{-1} is attributed to

carbonate group which is appeared also in BG-60% Ch and BG-90% Ch samples.

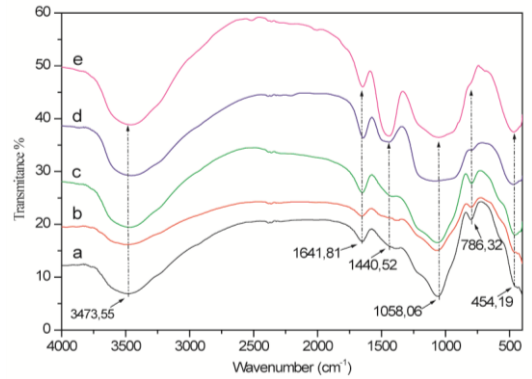


Fig. 4 FTIR spectra of bioactive glass powders 63S: (a) BG-0% Ch, (b) BG-10% Ch, (c) BG-30% Ch, (d) BG-60% Ch and (e) BG-90% Ch.

III.2.3. SEM analysis of bioactive glasses

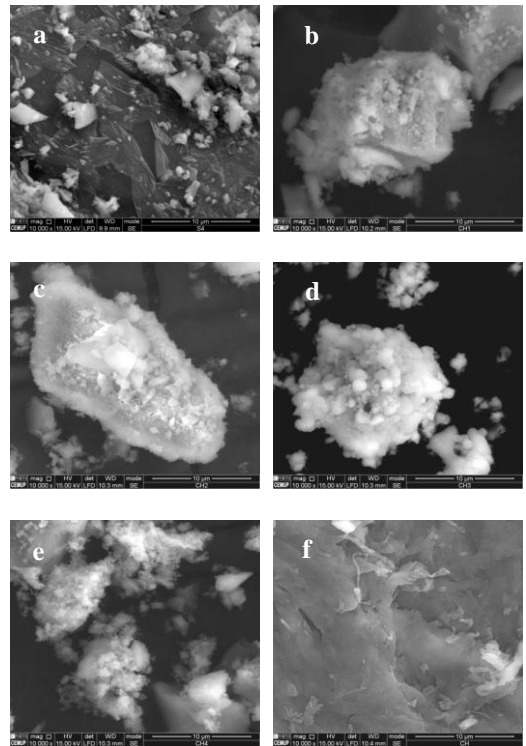


Fig. 5 Morphology of bioactive glass powders: (a) BG-0% Ch, (b) BG-10% Ch, (c) BG-30% Ch, (d) BG-60% Ch and (e) BG-90% Ch, (f) Chitosan (Ch).

The microstructure and the morphology of the bioactive glass powders shows on Fig.5 depends on the rate of the addition of the chitosan. The bioactive glass powder without addition of chitosan (BG-0%Ch) shows a very dense structure with almost zero porosity (Fig. 5a). Whereas, the powders with 10% (Fig. 5b) and 30% on chitosan (Fig. 5b and 5c) shown the same structure which is much similar to the BG-0%Ch with lower density. Powder with 60% chitosan (Fig. 5d) shown spherical particles agglomerated and bioactive glass powder with 90% chitosan (Fig. 5e) showed very small spherical particles with a sponge structure which indicate the crystalline nature of these two powders. These results are in agreement with the results of XRD studies (Fig. 3). Fig. 5f, shows the micrographs of chitosan with a smooth, compact, and homogeneous surface.

IV. CONCLUSION

Different rate of chitosan was added to the solution of bioactive glass precursors synthesized by sol-gel method. The results show that the addition of chitosan influenced the structure and morphology of bioactive glass powders obtained at a fixed sintering temperature of 600°C. X-ray diffraction analysis shows an amorphous structure of the bioactive glass powders with 0, 10 and 30 % of chitosan and a crystalline structure up to 30%. The crystallization process of the bioactive glass powders increased with increasing of the rate of chitosan and SEM analysis is in agreement with XRD analysis.

Références

[1]. Jose Renato J. Delben. Odair M. Pimentel. Marlene B. Coelho. Pollyanna D. Candelorio. Leonardo N. Furini. Fabio Alencar dos Santos. Fabio S. de Vicente. Qngela A.S.T. Delben. Synthesis and thermal properties of nanoparticles of bioactive glasses containing silver. *J Them Anal Calorim.* 97 (2009) 433-436.
 [2]. A. R. Curtis. N.X. West. B. Su. Synthesis of nanobioglass and formation of apatite rods to occlude exposed dentine tubules and eliminate hypersensitivity. *Acta Biomaterialia.* 6 (2010) 3740-3746.
 [3]. F. Braye. J.L. Irigaray. E. Jallot. H. Oudadesse. G. Weber. N. Deschamps. C. Deschamps. P. Frayssinet. P.

Tourermet. H. Tixier. S. Terve. J. Lefaivrell. A. Amirabad. Resorption kinetics of osseous substitute: natural coral and synthetic hydroxyapatite. *Biomaterials.* 17 (1996) 1345-1350.
 [4]. Shin-hee jun. Eun-Jung Lee. Se-Won Yook. Hyoun-Ee Kim. Hae-Won Kim. Young-Hag Koh. A bioactive coating of a silica xerogel/chitosan hybrid on titanium by a room temperature sol-gel process. *Acta Biomaterialia.* 6 (2010) 302-307.
 [5]. H. Oudadesse. E. Dietrich. X.V. Bui. Y. Le Gal. P. Pellen. G. Cathelineau. Enhancement of cells proliferation and control of bioactivity of strontium doped glass. *Applied Surface Science* 257 (2011) 8587- 8593.
 [6]. L.L. Hench. R.J. Splinter. W.C. Allen. T.K. Greenlee. Bonding mechanism at interface of ceramic prosthetic materials. *J. Biomed. Mater. Res.* 5 (1971) 117-141.
 [7]. A. Doostmohamadi. A. Monshi. M. H. Fathi. S. Karbasi. O. Braissant. Q. U. Daniels. Direct cytotoxicity evaluation of 63S bioactive glass and bone-derived hydroxyapatite particles using yeast model and human chondrocyte cells by microcalorimetry. *J Mater Sci: Mater Med.* 22 (2011) 2293-2300.
 [8]. A. Lopez-Sastre. J.M. Gonzalo-Orden. J.A.R. Altónaga. J.R. Altónaga. M.A. Orden. Coating titanium implants with bioglass and with hydroxyapatite. *International Orthopaedics.* 22 (1998) 380-383.
 [9]. Abeer M. El-Kady. Ebtsam A. Saad. Bothaina M. Abd El-Hady. Mohmmad M. Farag. Synthesis of silicate glass/poly(L-lactide) composite scaffolds by freeze-extraction technique: Characterization and in vitro bioactivity evaluation. *Ceramics International.* 36 (2010) 995-1009.
 [10]. A. Saboori, M. Rabiee, F. Moztarzadeh, M. Sheikhi, M. Tahriri, M. Karimi. Synthesis, characterization and in vitro bioactivity of sol-gel-derived SiO₂-CaO-P₂O₅-MgO bioglass. *Materials Science and Engineering C.* 29 (2009) 335-340.
 [11]. Christel P. A.T. Klein. Y. Abe. H. Hosono. K. de Groot. Different calcium, phosphate bioglass ceramics implanted in rabbit cortical bone. An interface study. *Biomaterials.* 5 (1984) 362-364.
 [12]. D. Zhitomirsky. J.A. Roether. A.R. Boccaccini. I. zhitomirsky. Electrophoretic deposition of bioactive glass/polymer composite coating with and without HA nanoparticle inclusions for biomedical applications. *Journal of Materials Processing Technology.* 209 (2009) 1853-1860.
 [13]. Ruilin Du. Jiang Chang. Preparation and characteriwation of bioactive sol-gel-derived Na₂Ca₂Si₃O₉. *Journal of Materials Science: Materials in Medicine.* 15 (2004) 1285-1289.
 [14]. Ahmed Bachar. Cyrille Mercier. Arnaud Tricoteaux. Anne Leriche. Claudine Follet. Mohamed Saadi. Stuart Hampshire. Effects of addition of nitrogen on bioglass properties and structure. *Journal of Non-Crystalline Solids.* 358 (2012) 693-701.
 [15]. Mehahd Mehdipour. Abdollah Afshar. A study of the electrophoretic deposition of bioactive glass-chitosan

- composite coating. *Ceramics International*. 38 (2012) 471-476.
- [16]. F. Pishibin, V. Mourino, J.B. Gilchris, D.W. McComb, S. Kreppel, V. Salih, M.P. Ryan, A.R. Boccaccini. Single- step electrochemical deposition of antimicrobial orthopaedic coating based on a bioactive glass/chitosan/nano-silver composite system. *Acta biomaterialia*. 9 (2013) 7469-7479.
- [17]. Shin-Hee Jun, Eun-Jung Lee, Se-Won Yook, Hyoun-Ee Kim, Hae-Won Kim, Young-hag Koh. A bioactive coating of silica xerogel/chitosan hybrid on titanium by a room temperature sol-gel process. *Acta biomaterialia*. 6 (2010) 302-307.
- [18]. Prerna P. Dhawade, Ramanand N. Jagtap. Characterization of the glass transition temperature of chitosan and its oligomers by temperature modulated differential scanning calorimetry. *Advances in Applied Science Research*. 3 (2012) 1372-1382.
- [19]. Douglas de Britto, Sergio Paulo Campana-Filho. Kinetics of the thermal degradation of chitosan. *Thermochimica Acta* 465 (2007) 73–82.
- [20]. Lachezar Radev. Katia Hristova. Valery Jordanov. Maria Helena V. Fernandes. Isabel Margarida M. Slvado. In vitro bioactivity of 70 Wt.% SiO₂- 30 Wt.% CaO sol-gel glass, doped with 1,3 and 5 Wt.% NbF₅. *Central European Journal of Chemistry*. 10 (2012) 137-145.
- [21]. Alberto Rainer. Sara Maria Giannitelli. Franca Abbruzzese. Enrico Traversa. Silvia Licoccia. Marcella Trombetta. Fabrication of bioactive glass-ceramic foams mimicking human bone portions for regenerative medicine. *Acta Biomaterialia*. 4 (2008) 362-369.
- [22]. J.Ma. C.Z. Chen. D.G. wang. X.G. Meng. J.Z. Shi. Influence of the sintering temperature on the structural feature and bioactivity of sol-gel derived SiO₂-CaO-P₂O₅ bioglass. *Ceramics International*. 36 (2010) 1911-1916.
- [23]. Anita Lucas-Girot. Fatima Zohra Mezahi. Mohamed Mami. Hassane Oudadesse. Abdelhamid Harabi. Marie Le Floch. Sol-gel synthesis of a new composition of bioactive glass in the quaternary system SiO₂-CaO-Na₂O-P₂O₅ Comparison with melting method. *Journal of Non-Crystalline Solids*. 357 (2011) 3322–3327.
- [24]. H.A. Elbatal. M.A. Azooz. E.M.A. Khalil. A. Soltan Monem. Y.M. hamdy. Characterization of some bioglass-ceramics. *Materials Chemistry and Physics*. 80 (2003) 599-609.
- [25]. M.H. Fathi. A/ Doostmohammadi. Bioactive glass nanopowder and bioglass coating for biocompatibility improvementt of metallic implant. *Journal of Materials Processing Technology*. 209 (2009) 1385-1391.
- [26]. E.V. tarasyuk. O. A. Shilova. A. M. Bochkin. A. D. Pomogailo. Investigation into the influence of organic modifiers and ultradispersed hybrid fillers on the structure and properties of glass-ceramic coating prepared by the sol-gel method. *Glass Physics and Chemistry*. 32 (2006) 439-447.
- [27]. J.P. Nayak. S. Kumar. J. Bera. Sol-gel synthesis of bioglass-ceramics using rice husk ash as a source for silica and its characterization. *Journal of Non-Crystalline Solids*. 356 (2010) 1447-1451.
- [28]. Hermes. S. Costa. Magda F. Rocha. Giovanna I. Andrade. Edel F. Barbosa-Stancioli. Marivalda M. Pereira. Rodrigo L. Orefice. Wander L. Vasconcelos. Herman S. Mansur. Sol-gel derived composite from bioactive glass-polyvinyl alcohol. *Journal of Materials Science*. 43 (2008) 494-502.